The HSP90 inhibitor ganetespib synergizes with the MET kinase inhibitor crizotinib in both crizotinib-sensitive and crizotinib-resistant MET-driven tumor models

Naoto Miyajima[1,3], Shinji Tsutsumi[1], Carole Sourbier[1], Kristin Beebe[1], Mehdi Mollapour[1,4], Candy Rivas[1], Soichiro Yoshida[1], Jane B. Trepel[2], Ying Huang[1], Manabu Tatokoro[1], Nobuo Shinohara[3], Katsuya Nonomura[3] and Len Neckers[1*]

[1]Urologic Oncology Branch and [2]Medical Oncology Branch, Center for Cancer Research, National Cancer Institute, National Institutes of Health, Bethesda, MD 20892; [3]Department of Urology, Hokkaido University Graduate School of Medicine, Sapporo 060-8638, Japan; [4]Departments of Urology, Biochemistry and Molecular Biology, Cancer Research Institute, SUNY Upstate Medical University, 750 E. Adams St., Syracuse, NY 13210, USA

[#]Corresponding author:

Len Neckers, PhD
Urologic Oncology Branch, National Cancer Institute, Building 10/CRC, room 1-5940, 9000 Rockville Pike, Bethesda, Maryland 20892
Phone: 301-496-5899; fax: 301-402-0922; e-mail: neckersl@mail.nih.gov

Running title: HSP90 inhibition reverses MET resistance to crizotinib

Keywords: Heat shock protein 90, MET, tyrosine kinase resistance, tumorigenesis

Word count (excluding references): 4,460

Total number of figures and tables: 6

There are no conflicts of interest to disclose for any of the authors of this manuscript.

Abstract

The proto-oncogene MET is aberrantly activated via overexpression or mutation in numerous cancers, making it a prime anti-cancer molecular target. However, the clinical success of MET-directed tyrosine kinase inhibitors (TKI) has been limited due, in part, to mutations in the MET kinase domain that confer therapeutic resistance. Circumventing this problem remains a key challenge to improving durable responses in patients receiving MET-targeted therapy. MET is an HSP90-dependent kinase, and in this report we show that HSP90 preferentially interacts with and stabilizes activated MET, whether the activation is ligand-dependent or is a consequence of kinase domain mutation. In contrast, many MET TKI show a preference for the inactive form of the kinase and activating mutations in MET can confer resistance. Combining the HSP90 inhibitor ganetespib with the MET TKI crizotinib achieves synergistic inhibition of MET, its downstream signaling pathways, and tumor growth in both TKI-sensitive and TKI- resistant MET-driven tumor models. These data suggest that inclusion of an HSP90 inhibitor can partially restore TKI sensitivity to previously resistant MET mutants, and they provide the foundation for clinical evaluation of this therapeutic combination in patients with MET-driven cancers.

Introduction

The proto-oncogene product MET is a receptor tyrosine kinase whose ligand is hepatocyte growth factor/scatter factor (HGF/SF). HGF binding to MET induces receptor dimerization and trans-phosphorylation, and promotes activation of several signaling networks including PI3K-AKT and MAPK-ERK pathways (1). Activating point mutations in the MET kinase domain are implicated in the etiology of hereditary papillary renal carcinoma and have also been detected in sporadic papillary renal carcinoma, lung cancer and gastric cancer (2-5). Furthermore, amplification of the *MET* gene locus has been detected in patients with gastric and metastatic colorectal cancers (6, 7). Cell lines engineered to express high levels of wild-type MET or constitutively active mutant MET display a proliferative, motogenic, and invasive phenotype, and form metastatic tumors in nude mice (8-11).

MET is a validated molecular target for cancer therapy, and MET tyrosine kinase inhibitors (TKIs) represent a promising treatment modality. Crizotinib, an orally available ATP-competitive and selective small-molecule inhibitor of MET, exhibits marked antitumor activity in several MET-dependent xenograft models (12). A recent Phase II study of the dual MET/VEGFR2 inhibitor foretinib in patients with papillary renal cell carcinoma reported an overall response rate (using Response Evaluation Criteria in Solid Tumors 1.0) of 13.5 %, and the presence of a germline MET mutation was highly predictive of a response (13). However, recent studies suggest that primary (*de novo*) resistance to TKI is likely be encountered in tumors harboring certain activating MET mutations. Thus, although crizotinib can inhibit the activity of most MET mutants, some constitutively active mutants, including MET-L1213V and -Y1248H, are resistant to this inhibitor (12, 14). Additional studies have suggested that

these mutations not only mediate primary resistance to MET inhibitors but may also play a role in acquired resistance to MET TKI (15-17).

Heat shock protein 90 (HSP90) is a molecular chaperone whose association is required for the stability and function of multiple mutated or overexpressed signaling proteins, including many kinases, that promote the growth and survival of cancer cells. Small molecule HSP90 inhibitors cause HSP90 to dissociate from its clients, resulting in their destabilization and eventual degradation. HSP90 inhibitors have been validated in numerous preclinical tumor models and have shown promising activity in several clinical trials (18-20).

HSP90 inhibitors have been reported to destabilize MET (21, 22), as well as several MET-activated downstream signaling proteins, including AKT and RAF (23-25). Based on these findings, HSP90 inhibitors are expected to effectively interdict MET signaling at multiple points to inhibit the proliferation of MET-driven cancer cells. Indeed, the HSP90 inhibitors ganetespib (STA-9090) and SNX-2112 have each shown potent activity in several preclinical MET-driven tumor models, including those resistant to MET TKI (26, 27). However, a detailed study of the MET-HSP90 interaction and its role in supporting MET activation has not been reported, nor has the possible synergy between HSP90 inhibition and MET TKI been rigorously examined.

In the current study, we show that HSP90 interacts preferentially with activated MET, whether activation depends on HGF engaging the receptor or is mediated by kinase domain mutation. Further, we show that the activated MET fraction is most sensitive to HSP90 inhibition. The HSP90 inhibitor ganetespib displays synergy, both *in vitro* and *in vivo*, with the MET TKI crizotinib in cells overexpressing wild-type MET. Unexpectedly, low-dose ganetespib also partially restores crizotinib sensitivity, *in vitro*

and *in vivo*, to cells and tumors expressing TKI-resistant MET mutants. Our findings support the use of HSP90 inhibitors to overcome or delay the initiation of resistance to MET TKI, and they provide the basis for clinical evaluation of this combination in patients with MET-driven cancers.

Materials and Methods

Cell lines. MKN45, H1993 and HEK293 cell lines (American Type Culture Collection) were maintained under 5% CO_2 at 37°C in either RPMI 1640 (MKN45, H1993), or DMEM (HEK293) supplemented with 10% FBS. NIH3T3 cell lines stably expressing either wild type or mutant MET proteins (V1238I, H1112Y, Y1248H, L1213V, M1268T and V1110I) were kindly provided by Dr. Laura Schmidt (NCI, Bethesda, MD, USA). These cells were cultured in DMEM with 10% FBS and 0.5 mg/ml G-418.

Antibodies and reagents. Antibodies to MET, phospho-Tyr1234/35 MET, Akt, phospho-Ser473 Akt, Erk1/2, phospho-Thr202/Tyr204 Erk1/2 (Cell Signaling), HSP90 (StressGen), V5 (Invitrogen), ubiquitin (Santa Cruz), α-tubulin (Calbiochem) were used for immunoprecipitation and/or immunoblotting. Geldanamycin was obtained from the Developmental Therapeutics Program, NCI. Ganetespib and crizotinib were obtained from Synta Pharmaceuticals. Mouse IgG, MG132 and recombinant human HGF were purchased from Millipore, Sigma and R&D Systems, respectively. FuGene6 (Roche) was used for transient transfection.

Immunoprecipitation and immunoblotting. These experiments were performed as previously described (28). Briefly, cells were lysed in buffer containing 20 mM Hepes, 100 mM NaCl, 1 mM $MgCl_2$, 0.1% Nonidet P-40, 20 mM Na_2MoO_4, phosphatase and protease inhibitors. Immunoprecipitates or cell lysates were resolved by 4–20% SDS/PAGE, transferred to nitrocellulose membrane, and probed with respective antibodies.

Plasmid constructs. Human MET cDNA was kindly provided by Dr. Don Bottaro (NCI, Bethesda, MD, USA). Chimeric mutant MET/EGFR was generated using PCR and ligated into pcDNA vector (Invitrogen) in-frame with the C-terminal V5 tag. Point

mutation was made using QuikChange (Stratagene) according to the manufacturer's instructions.

Cell proliferation assay. Cells were seeded in 96-well plates at 5,000 per well and incubated for 24 h, followed by addition of drugs. After 48 h, MTT solution (Sigma) was added and plates were allowed to incubate at 37°C for 3 h. Optical density at 570 nm was determined by spectrophotometer (Bio-TEK). Combination index (CI) was calculated by the median-effect method of Chou and Talalay (29) using CalcuSyn software (Biosoft).

Cell cycle analysis. Cells were plated at a density of 3×10^5 in 10 cm dishes and incubated for 24 h, followed by addition of drugs. After 48 h, cells were fixed with 70% ethanol for 4 h at -20°C, and then suspended in a solution containing 0.04% digitonin. Cells were incubated at 37°C for 1 h in a solution containing RNase A (100 μg/mL; Novagen) and propidium iodide (50 μg/mL) and then analyzed with a FACSCalibur flow cytometer (Becton Dickinson).

Colony formation assay. Cells were plated at a density of 1×10^4 in 60 mm dishes containing 0.4% top low-melting agarose and 0.5% bottom low-melting agarose medium and cultured for 3 weeks. Colonies with a diameter of > 0.1 mm were counted in 5 random high-power fields.

Migration and invasion assay. Twelve-well polycarbonate transwell chambers with 8 μm pores (Corning) coated with with matrigel (BD Biosciences) were used. Cells (1×10^5) were added to the upper well in serum-free medium with indicated drugs. In the lower well, medium with 10% FBS was used as chemo-attractant. After 48 h, cells on the upper surface of the filter were carefully removed with cotton pads. Migrated cells were fixed in 3.7% formaldehyde and stained with DAPI. Invaded cells were fixed and

stained with Diff-Quik Stain kit (Dade Behring). The number of cells in 5 random high-power fields was determined.

Animal experiments. Animal experiments and procedures were carried out in accordance with the Guide for the Care and Use of Laboratory Animals as adopted and promulgated by the National Institutes of Health. To establish tumor xenografts, cells (1 x 10^6) were injected into the flank of female Nu/Nu mice (6 weeks of age, Taconic). After tumors reached a mean volume of 100 mm^3, mice were administered crizotinib in water by oral gavage or ganetespib in 10/18 DRD (10% DMSO, 18% Cremophor RH40, 3.6% dextrose in water) by intraperitoneal injection. Tumor volume was calculated as the product of length x $width^2$ x 0.5. Fractional tumor volume (FTV) relative to untreated controls was determined as described previously (30). On the final day of the study, mice were humanely euthanized and tumors were resected and pulverized using a homogenizer (Kinematica). Protein lysates were subjected to immunoblotting.

Statistical analysis. To determine statistical significance of experimental data, we used the unpaired Student's *t*-test followed by Bonferroni post hoc test for multiple comparisons. Data represent the mean ± SD. All P values < 0.05 were considered statistically significant relative to control and designated with an asterisk (*). Statistical analysis was done with JMP software (SAS Institute).

Results

Wild-type MET is an HSP90-dependent kinase.

We assessed the interaction of HSP90 and wild-type MET (wtMET) in the gastric cancer cell line MKN45, which overexpresses wtMET. As shown in Figure 1*A*, endogenous HSP90 coprecipitated, albeit weakly, with wtMET. Previous reports by us and others have suggested that the activated states of some HSP90-dependent kinases have a greater dependence on HSP90 (31-33). To determine if this were the case for MET, we compared the degree of wtMET/HSP90 interaction in the presence and absence of the MET ligand HGF. Co-immunoprecipitation of HSP90 with MET clearly increased upon HGF stimulation and correlated with an increased population of activated (phosphorylated) MET (Figure 1*B*). Next, we compared the sensitivity of total and activated wtMET protein to HSP90 inhibition. Exposure of MKN45 cells to the HSP90 inhibitor geldanamycin (GA) reduced the steady-state expression of both total and activated MET protein in a dose- and time-dependent manner, but the activated MET fraction was most sensitive to HSP90 inhibition (Figure 1*C*). Loss of MET protein expression occurred much more rapidly in the presence of GA than following inhibition of protein synthesis with cycloheximide (Figure S*1B*, MKN45 panels), supporting Hsp90 inhibitor-mediated destabilization of activated MET. Next, we determined whether HSP90 inhibition promotes wtMET ubiquitination and degradation by the proteasome, a common fate of most HSP90 clients deprived of interaction with the chaperone (34). Co-treatment with the proteasome inhibitor MG132 reversed the impact of HSP90 inhibition on steady-state expression of activated MET (Figure 1*D*), while brief exposure of MKN45 cells to GA increased MET ubiquitination and this was further enhanced by co-treatment with proteasome inhibitor (Figure 1*E*).

HSP90 preferentially associates with activated MET.

These data suggest that HSP90 interacts preferentially with and stabilizes the activated fraction of MET. In contrast to wtMET, which requires HGF binding for stimulation of its kinase activity, MET proteins with specific mutations in the kinase domain display constitutive activity in the absence of HGF. Therefore, we asked whether HSP90 also interacted robustly with a constitutively active MET mutant. To maintain a similar cell background, we immunoprecipitated MET from NIH3T3 cells stably expressing either wt MET or the constitutively active MET mutant Y1248H. HSP90 association with MET-Y1248H was markedly increased compared to wtMET (in the absence of exogenous HGF), in accordance with the different steady state activation states of these MET proteins (Figure 2*A*). Next, we compared the sensitivity of wtMET and the constitutively active MET-Y1248H mutant to GA. In stably transfected NIH3T3 cells, we found MET-Y1248H (both activated and total) to be more sensitive to Hsp90 inhibition compared to wtMET (Figure *2B*).

Consistent with these data, activated MET-Y1248H is robustly protected from GA by co-treatment with the proteasome inhibitor MG132 (Figure *S1A*). Like activated wtMET, loss of activated MET-1248H protein expression occurred much more rapidly in the presence of GA than after protein synthesis inhibition (Figure S*1B*). Taken together, these data suggest that Hsp90-mediated stabilization of activated MET is required for optimal MET kinase activity. To provide further support for this hypothesis, we examined the ability of constitutively active MET-Y1248H to phosphorylate its substrate Gab1 (35) in NIH3T3/MET-Y1248H cells treated with the Hsp90 inhibitor ganetespib (Figure S*2A*). Importantly, Gab1 is not an Hsp90 client and total endogenous Gab1 expression was not affected by ganetespib treatment. Nonetheless, ganetespib

caused a dose-dependent reduction of Gab1 phosphorylation in these cells.

To better understand where HSP90 interacts with MET and how it might affect its kinase activity, we examined the αC-β4 loop located in the MET kinase domain. Amino acid composition of this short loop was shown to be important for HSP90 binding to a number of kinases including ErbB2 (36, 37). We reported previously that although the kinase domains of HSP90-dependent ErbB2 and HSP90-independent EGFR (ErbB1) are highly homologous, they vary in sequence in the αC-β4 loop. Replacement of the αC-β4 loop in ErbB2 with that of the EGFR abrogated HSP90 binding, while replacing the EGFR αC-β4 loop with that of ErbB2 conferred Hsp90 association and dependence (37). When we compared the sequence of the αC-β4 loops in EGFR and MET, we found a divergence in 8 of 10 residues between amino acids 1132 and 1141 (numbering for MET kinase domain residues; highlighted in grey, Figure 2*C*). To investigate whether these residues are an important determinant of MET/HSP90 interaction, we replaced the 8 divergent residues in V5-tagged MET-Y1248H with those found in the αC-β4 loop of the EGFR (V5-MET-Y1248H/EGFR, highlighted in red, Figure 2*C*). After transient transfection into HEK293 cells, we immunoprecipitated the tagged MET proteins with antibody to V5 and we assessed the relative association of both MET-Y1248H and MET-Y1248H/EGFR with HSP90. Although V5 immunoprecipitation affinity-purified equivalent amounts of tagged MET proteins from cell lysates, co-immunoprecipitated HSP90 was present in only trace amounts in MET-Y1248H/EGFR immune pellets. This was in distinct contrast to the amount of HSP90 found associating with MET-Y1248H protein (Figure 2*D*), confirming that amino acid composition of the αC-β4 loop in the MET kinase domain determines HSP90 association.

We noticed that, concurrent with loss of HSP90 association, the activated fraction of immunoprecipitated MET-Y1248H/EGFR was dramatically reduced compared to MET-Y1248H. To confirm this result, we blotted equivalent amounts of protein lysate from the transfected cells with antibody to phospho-MET. Substitution of the αC-β4 loop in MET-Y1248H nearly completely abrogated its constitutive phosphorylation (Figure 2*E*). To ascertain whether reduced constitutive activation also reflected an inability to respond to ligand, we compared the ability of HGF to activate MET-Y1248H/EGFR and wtMET in transiently transfected serum-starved HEK293 cells. The data show that although constitutive phosphorylation of MET-Y1248H/EGFR is even less than that of wtMET (Figure 2F, 'HGF –' lanes), both proteins are comparably activated by HGF (Figure 2F, 'HGF +' lanes). Further, we found MET-Y1248H/EGFR to be more sensitive to crizotinib compared to MET-Y1248H (Figure *2G*), supporting an inverse correlation between Hsp90 interaction and crizotinib sensitivity. This hypothesis is consistent with *in vitro* data showing that the TKI sensitivity of constitutively active, bacterially expressed MET-Y1248D protein is antagonized by pre-incubation with purified Hsp90 prior to *in vitro* kinase assay. In contrast, inclusion of GA restores sensitivity to MET TKI *in vitro* (Figure *S2B*).

The MET inhibitor crizotinib synergizes *in vitro* with ganetespib in wtMET-driven cells.

Most MET TKIs are ATP-competitive inhibitors and preferentially target the inactive form of MET (38). In contrast, the data presented here show that HSP90 inhibitors appear to preferentially target activated MET and, at least *in vitro*, appear to enhance sensitivity of activated MET to TKI. To determine whether a similar phenomenon occurs in cells, we first assessed the effect of the MET TKI crizotinib and of the second

generation HSP90 inhibitor ganetespib, alone or combined, on the activation state of wtMET, and on downstream signaling to AKT and ERK1/2 in the wtMET-overexpressing gastric carcinoma cell line MKN45 and the non-small cell lung carcinoma cell line H1993. In both cell lines, addition of low-dose ganetespib dramatically enhanced the impact of crizotinib on the activation of all three kinases (Figure 3*A*). Although AKT itself is an HSP90 client, the lowest dose of ganetespib (10 nM) had minimal activity when used alone in either cell line.

To investigate whether enhanced inhibition of these signaling pathways correlated with enhanced cellular activity, we performed MTT assays using MKN45 cells. Addition of increasing concentrations of ganetespib to a fixed set of crizotinib concentrations shifted the dose-response curves to the left in a (ganetespib) concentration-dependent manner (Figure 3*B*), suggesting that combination of these two drugs might be synergistic. We confirmed this to be the case by calculating the combination index (CI) using the median-effect method of Chou and Talalay (29). CI values under 1 indicate synergy, whereas CI values over 1 reflect antagonism. Based on these data, ganetespib and crizotinib clearly synergize in MKN45 cells (CI = 0.6, Figure 3*C*). Cell cycle analysis revealed an increase in G1 phase in ganetespib/crizotinib treated cells (as well as a small increase in sub-G1), and this was not observed in cells treated with either drug alone (Figure 3*D*).

Next, we determined the effect of combination therapy on the transformed phenotype of MKN45 cells by assessing anchorage-independent colony formation. Low-dose crizotinib (10 nM) and ganetespib (10 nM) alone had marginal effects on colony formation. However, combination of both drugs inhibited MKN45 colony formation by more than 90% (Figure 3*E*). Combination treatment also more effectively

inhibited MKN45 cell migration, compared with single agent treatment at equivalent concentrations (Figure S*3*).

Crizotinib-resistant MET mutants retain sensitivity to Hsp90 inhibition.

De novo or acquired resistance to MET TKI as a consequence of MET mutation remains a key therapeutic challenge to the clinical utility of these drugs. Several germline and somatic mutations in the tyrosine kinase domain of MET have been identified in hereditary papillary renal cancers and these tumors are MET-driven (5, 13). A majority of these MET mutants are constitutively active and some demonstrate *de novo* resistance to MET TKI (9, 39). Since MET activity depends on association with HSP90, we speculated that HSP90 inhibitors might also retain activity towards a range of MET mutants, including those that are TKI-resistant. To examine this possibility, we compared the inhibitory activity of single agent crizotinib with that of single agent ganetespib in six MET mutants, four that retain TKI sensitivity (MET-V1238I, MET-H1112Y, MET-M1268T, and MET-V1110I) and two that are resistant to MET inhibitors (MET-Y1248H and MET-L1213V). For TKI-sensitive mutants, both MET phosphorylation and the activity of downstream signaling pathways (pAKT and pERK) were equally or more potently inhibited by ganetespib than by crizotinib (Figure 4*A* and Figure S*4*). However, in contrast to crizotinib, ganetespib retained equivalent or greater inhibitory activity in TKI-resistant mutants compared to wtMET (Figure 4*B*).

Given these data and in light of the synergy we observed for wtMET, we investigated next whether combining crizotinib and ganetespib might provide a therapeutic benefit in MET TKI-resistant cells. Indeed, although crizotinib alone below 0.5 μM did not affect MET phosphorylation and downstream signaling in TKI-resistant MET-Y1248H expressing NIH3T3 cells, low concentrations of ganetespib (10 nM and

20 nM, see also Figure 4*B*) together with crizotinib (0.25 μM) dramatically decreased pMET, pAKT and pERK1/2 when compared to these concentrations of ganetespib alone (Figure 5*A*). We observed similar results for TKI-resistant MET-L1213V expressing NIH3T3 cells, suggesting that low-dose ganetespib can partially re-sensitize MET TKI-resistant cells to crizotinib. To further examine this hypothesis, we assessed colony formation using MET-Y1248H-expressing NIH3T3 cells. Although at the concentrations chosen, neither crizotinib (200 nM) nor ganetespib (10 nM) individually affected colony formation, when combined they dramatically inhibited the anchorage-independent growth of these cells (Figure 5*B*). Indeed, with a calculated CI of < 1 (see Table *S1*), the combined activity of both drugs in this assay reflects synergy. Combination therapy also significantly inhibited the invasive capability of MET-Y1248H expressing NIH3T3 cells at dose levels that were ineffective when administered separately (Figure 5*C*). These *in vitro* data suggest that combining ganetespib with crizotinib provides at least an additive therapeutic benefit in MET TKI-resistant cells.

HSP90 inhibition synergizes *in vivo* with MET TKI, even in MET TKI-resistant xenografts.

In order to determine whether there may be therapeutic benefit in combining ganetespib with crizotinib *in vivo*, we employed two distinct xenograft models. MKN45 xenografts (expressing wtMET) were sensitive to MET TKI (91% inhibition of tumor growth 36 days after tumor inoculation in mice treated daily with 50 mg/kg crizotinib) in agreement with previous reports (12, 27), while MET-Y1248H NIH3T3 xenografts were predictably MET TKI-resistant (59% inhibition of tumor growth at 21 days after daily treatment with 150 mg/kg crizotinib) (Figure S*5*). In contrast, ganetespib was

effective in both xenograft models, although at the maximum dose used in this study (50 mg/kg administered 3x per week), somewhat greater activity was seen in wtMET xenografts (95% inhibition of tumor growth) compared to MET-Y1248H xenografts (82% growth inhibition) (Figure S*5*).

To evaluate whether combination therapy was beneficial in the MKN45 model, we chose crizotinib (12.5mg/kg) and ganetespib (12.5 mg/kg) dosing that provided approximately 50% growth inhibition when used singly (Figure S*5*). Treatment with this drug combination proved to be significantly more potent (95% growth inhibition) compared to single agent treatment (56% growth inhibition for crizotinib alone and 64% growth inhibition for ganetespib alone) (Figure 6*A*).

In mice bearing TKI-resistant MET-Y1248H xenografts, we similarly observed that combination therapy with ganetespib and crizotinib (37.5 mg/kg and 125 mg/kg, respectively) inhibited tumor growth by 90%, which was significantly greater than the inhibition achieved by treating with either drug alone (65% growth inhibition for ganetespib and 31% growth inhibition for crizitonib) (Figure 6*B*).

Based on comparison of expected and obtained fractional tumor volumes (FTV) in single agent-treated and combination-treated mice (30), crizotinib and ganetespib synergized to inhibit both wtMET-driven and TKI-resistant MET (Y1248H)-driven xenograft growth (Table *S2*). None of the drug regimens significantly affected animal body weight in either xenograft model (Figure 6*A*, *B*). In agreement with these tumor growth data, the impact of combination therapy on tumor MET activation status and downstream signaling pathways was greater than single agent treatment in both xenograft models, recapitulating the *in vitro* data described earlier (Figure 6*C*, *D*).

Discussion

Although small molecule kinase inhibitors have demonstrated clinical efficacy in cancer, patients who initially respond to such targeted therapy frequently will develop resistance. Mechanisms of resistance include the growth advantage provided by appearance of drug resistant kinase mutations (40), as well a process termed ‘‘oncogene switching’’ whereby TKI-treated cells utilize an alternative kinase to drive shared downstream signaling pathways (41). Recent studies have revealed that HSP90 inhibition can overcome both forms of kinase inhibitor resistance. For example, HSP90 inhibition suppresses EGFR activity and downstream signaling in erlotinib-resistant EGFR/T790M-expressing cells (42), and suppresses ALK activity and signaling in cells expressing crizotinib-resistant EML4-ALK/L1196M (43). Likewise, targeting HSP90 prevents escape of ErbB2-driven breast cancer cells from chronic ErbB inhibition and escape of MET-amplified tumor cells from MET TKI (44, 45).

TKI-resistance conferring MET kinase domain mutations, including Y1248H and L1213V, have been identified in hereditary papillary renal cell carcinomas (14), and long-term exposure to MET TKI *in vitro* leads to acquisition of these mutations in MET-expressing gastric cancer cells (15, 16). Such kinase activating mutations are thought to interfere with ATP-competitive TKI binding, and they likely contribute to both primary and acquired drug resistance in MET-dependent cancers. We have shown that a panel of MET proteins (both TKI-sensitive and TKI–resistant) retains dependence on HSP90 and remains sensitive to HSP90 inhibition. Importantly, we show that the active state of MET displays the strongest dependence on HSP90, whether activation is induced by HGF or is a consequence of kinase domain mutation (ligand-independent).

Because of the preference of HSP90 for activated MET, these data suggest the

possibility that HSP90 inhibition might synergize with MET TKI. Recent preclinical evaluation of the effects obtained upon simultaneously exposing acute myelogenous leukemia cells expressing activated FLT3 tyrosine kinase to both a FLT3-directed TKI and a HSP90 inhibitor lends support to this possibility, as does a recent study reporting the combinatorial benefit of ganetespib, crizotinib and other TKI in the context of EML4- ALK driven non-small cell lung cancer (46), (47). Our data show that simultaneous treatment with MET TKI and HSP90 inhibitor causes a true synergistic inhibition of cell growth in wild-type MET-expressing MKN45 gastric cancer cells. Synergy of this drug combination in these cells was reflected by enhanced inhibition of downstream signaling pathways, significantly greater inhibition of colony growth and cell motility, and by significantly greater growth inhibition of MKN45 xenografts *in vivo*.

Unexpectedly, we found that HSP90 inhibition also partially restored crizotinib sensitivity to two TKI-resistant MET mutants. Combination treatment dramatically inhibited MET signaling, colony growth, cell invasion, and xenograft growth *in vivo*. While some of these effects may be due to inhibition of additional HSP90 clients functioning within or parallel to MET-driven signaling pathways, the data we have presented here indicate that, at least for MET, HSP90 inhibition directly affects MET sensitivity to a TKI. Our model is in general agreement with a recent study proposing that TKI binding stabilizes HSP90-dependent kinases and obviates the need for HSP90 interaction (48), since we have shown that it is the activated state of MET that interacts most strongly with and is most dependent on HSP90. Another report has suggested that TKI binding promotes kinase degradation by denying access to HSP90 (49), although in the case of MET it appears that this would be the case only if the TKI bound to the

active conformation of the kinase, promoted dissociation of HSP90 and limited a return to the inactive conformation. The unexpected combinatorial benefit we have shown for TKI-resistant MET highlights the complex influence of HSP90 on kinase conformation, especially in the context of activating mutations, and our model provides a rationale for the increased dependence of other constitutively active kinase mutations on HSP90. For example, others have shown that HSP90 inhibitor synergizes with a Bcr-Abl TKI in TKI-resistant chronic myelogenous leukemia cells (50). While the benefit of simultaneous treatment with TKI and HSP90 inhibitor should be evaluated on a case by case basis, a rationale for such a strategy clearly exists in certain settings. Specifically, our data suggest that a MET/HSP90 inhibitor combination regimen is a viable strategy to be explored in patients with naïve MET-dependent cancers, as well in those patients whose cancers have developed resistance to MET TKI. While delaying or reversing MET TKI resistance, an effective MET/HSP90 inhibitor combination strategy may also require lower (and thus potentially less toxic) concentrations of both drugs.

Acknowledgments

We thank Y.H. Lee and D. Bottaro for V5-tagged plasmids, human MET cDNA and for helpful discussions. We also thank L. Schmidt for MET mutants, mutant MET-expressing NIH3T3 cells, careful reading of the manuscript and for helpful discussions. This study was supported by funds from the Intramural Research Program, National Cancer Institute, Center for Cancer Research. Ganetespib and crizotinib were provided by W. Ying, Synta Pharmaceuticals, Inc.

References

1. Birchmeier C, Birchmeier W, Gherardi E, Vande Woude GF. Met, metastasis, motility and more. Nat Rev Mol Cell Biol. 2003;4:915-25.

2. Di Renzo MF, Olivero M, Martone T, Maffe A, Maggiora P, Stefani AD, et al. Somatic mutations of the MET oncogene are selected during metastatic spread of human HNSC carcinomas. Oncogene. 2000;19:1547-55.

3. Lee JH, Han SU, Cho H, Jennings B, Gerrard B, Dean M, et al. A novel germ line juxtamembrane Met mutation in human gastric cancer. Oncogene. 2000;19:4947-53.

4. Ma PC, Kijima T, Maulik G, Fox EA, Sattler M, Griffin JD, et al. c-MET mutational analysis in small cell lung cancer: novel juxtamembrane domain mutations regulating cytoskeletal functions. Cancer Res. 2003;63:6272-81.

5. Schmidt L, Duh FM, Chen F, Kishida T, Glenn G, Choyke P, et al. Germline and somatic mutations in the tyrosine kinase domain of the MET proto-oncogene in papillary renal carcinomas. Nat Genet. 1997;16:68-73.

6. Di Renzo MF, Olivero M, Giacomini A, Porte H, Chastre E, Mirossay L, et al. Overexpression and amplification of the met/HGF receptor gene during the progression of colorectal cancer. Clin Cancer Res. 1995;1:147-54.

7. Kuniyasu H, Yasui W, Kitadai Y, Yokozaki H, Ito H, Tahara E. Frequent amplification of the c-met gene in scirrhous type stomach cancer. Biochem Biophys Res Commun. 1992;189:227-32.

8. Jeffers M, Rong S, Anver M, Vande Woude GF. Autocrine hepatocyte growth factor/scatter factor-Met signaling induces transformation and the invasive/metastastic phenotype in C127 cells. Oncogene. 1996;13:853-6.

9. Jeffers M, Schmidt L, Nakaigawa N, Webb CP, Weirich G, Kishida T, et al. Activating mutations for the met tyrosine kinase receptor in human cancer. Proc Natl Acad Sci U S A. 1997;94:11445-50.

10. Rong S, Bodescot M, Blair D, Dunn J, Nakamura T, Mizuno K, et al. Tumorigenicity of the met proto-oncogene and the gene for hepatocyte growth factor. Mol Cell Biol. 1992;12:5152-8.

11. Rong S, Segal S, Anver M, Resau JH, Vande Woude GF. Invasiveness and metastasis of NIH 3T3 cells induced by Met-hepatocyte growth factor/scatter factor autocrine stimulation. Proc Natl Acad Sci U S A. 1994;91:4731-5.

12. Zou HY, Li Q, Lee JH, Arango ME, McDonnell SR, Yamazaki S, et al. An orally available small-molecule inhibitor of c-Met, PF-2341066, exhibits

cytoreductive antitumor efficacy through antiproliferative and antiangiogenic mechanisms. Cancer Res. 2007;67:4408-17.

13. Choueiri TK, Vaishampayan U, Rosenberg JE, Logan TF, Harzstark AL, Bukowski RM, et al. Phase II and biomarker study of the dual MET/VEGFR2 inhibitor foretinib in patients with papillary renal cell carcinoma. J Clin Oncol. 2013;31:181-6.

14. Berthou S, Aebersold DM, Schmidt LS, Stroka D, Heigl C, Streit B, et al. The Met kinase inhibitor SU11274 exhibits a selective inhibition pattern toward different receptor mutated variants. Oncogene. 2004;23:5387-93.

15. Funakoshi Y, Mukohara T, Tomioka H, Ekyalongo RC, Kataoka Y, Inui Y, et al. Excessive MET signaling causes acquired resistance and addiction to MET inhibitors in the MKN45 gastric cancer cell line. Invest New Drugs. 2013.

16. Qi J, McTigue MA, Rogers A, Lifshits E, Christensen JG, Janne PA, et al. Multiple mutations and bypass mechanisms can contribute to development of acquired resistance to MET inhibitors. Cancer Res. 2011;71:1081-91.

17. Tiedt R, Degenkolbe E, Furet P, Appleton BA, Wagner S, Schoepfer J, et al. A drug resistance screen using a selective MET inhibitor reveals a spectrum of mutations that partially overlap with activating mutations found in cancer patients. Cancer Res. 2011;71:5255-64.

18. Neckers L, Workman P. Hsp90 molecular chaperone inhibitors: are we there yet? Clin Cancer Res. 2012;18:64-76.

19. Taldone T, Gozman A, Maharaj R, Chiosis G. Targeting Hsp90: small-molecule inhibitors and their clinical development. Curr Opin Pharmacol. 2008;8:370-4.

20. Whitesell L, Mimnaugh EG, De Costa B, Myers CE, Neckers LM. Inhibition of heat shock protein HSP90-pp60v-src heteroprotein complex formation by benzoquinone ansamycins: essential role for stress proteins in oncogenic transformation. Proc Natl Acad Sci U S A. 1994;91:8324-8.

21. Maulik G, Kijima T, Ma PC, Ghosh SK, Lin J, Shapiro GI, et al. Modulation of the c-Met/hepatocyte growth factor pathway in small cell lung cancer. Clin Cancer Res. 2002;8:620-7.

22. Webb CP, Hose CD, Koochekpour S, Jeffers M, Oskarsson M, Sausville E, et al. The geldanamycins are potent inhibitors of the hepatocyte growth factor/scatter factor-met-urokinase plasminogen activator-plasmin proteolytic network. Cancer Res. 2000;60:342-9.

23. Sato S, Fujita N, Tsuruo T. Modulation of Akt kinase activity by binding to

Hsp90. Proc Natl Acad Sci U S A. 2000;97:10832-7.

24. Schulte TW, Blagosklonny MV, Romanova L, Mushinski JF, Monia BP, Johnston JF, et al. Destabilization of Raf-1 by geldanamycin leads to disruption of the Raf-1-MEK-mitogen-activated protein kinase signalling pathway. Mol Cell Biol. 1996;16:5839-45.

25. Xu W, Yuan X, Jung YJ, Yang Y, Basso A, Rosen N, et al. The heat shock protein 90 inhibitor geldanamycin and the ErbB inhibitor ZD1839 promote rapid PP1 phosphatase-dependent inactivation of AKT in ErbB2 overexpressing breast cancer cells. Cancer Res. 2003;63:7777-84.

26. Bachleitner-Hofmann T, Sun MY, Chen CT, Liska D, Zeng Z, Viale A, et al. Antitumor activity of SNX-2112, a synthetic heat shock protein-90 inhibitor, in MET-amplified tumor cells with or without resistance to selective MET Inhibition. Clin Cancer Res. 2011;17:122-33.

27. Ying W, Du Z, Sun L, Foley KP, Proia DA, Blackman RK, et al. Ganetespib, a unique triazolone-containing Hsp90 inhibitor, exhibits potent antitumor activity and a superior safety profile for cancer therapy. Mol Cancer Ther. 2012;11:475-84.

28. Tsutsumi S, Mollapour M, Prodromou C, Lee CT, Panaretou B, Yoshida S, et al. Charged linker sequence modulates eukaryotic heat shock protein 90 (Hsp90) chaperone activity. Proc Natl Acad Sci U S A. 2012;109:2937-42.

29. Chou TC. Drug combination studies and their synergy quantification using the Chou-Talalay method. Cancer Res. 2010;70:440-6.

30. Yokoyama Y, Dhanabal M, Griffioen AW, Sukhatme VP, Ramakrishnan S. Synergy between angiostatin and endostatin: inhibition of ovarian cancer growth. Cancer Res. 2000;60:2190-6.

31. da Rocha Dias S, Friedlos F, Light Y, Springer C, Workman P, Marais R. Activated B-RAF is an Hsp90 client protein that is targeted by the anticancer drug 17-allylamino-17-demethoxygeldanamycin. Cancer Res. 2005;65:10686-91.

32. Li R, Soosairajah J, Harari D, Citri A, Price J, Ng HL, et al. Hsp90 increases LIM kinase activity by promoting its homo-dimerization. FASEB J. 2006;20:1218-20.

33. Xu W, Soga S, Beebe K, Lee MJ, Kim YS, Trepel J, et al. Sensitivity of epidermal growth factor receptor and ErbB2 exon 20 insertion mutants to Hsp90 inhibition. Br J Cancer. 2007;97:741-4.

34. Mimnaugh EG, Chavany C, Neckers L. Polyubiquitination and proteasomal degradation of the p185c-erbB-2 receptor protein-tyrosine kinase

induced by geldanamycin. J Biol Chem. 1996;271:22796-801.
35. Furge KA, Zhang YW, Vande Woude GF. Met receptor tyrosine kinase: enhanced signaling through adapter proteins. Oncogene. 2000;19:5582-9.
36. Citri A, Harari D, Shohat G, Ramakrishnan P, Gan J, Lavi S, et al. Hsp90 recognizes a common surface on client kinases. J Biol Chem. 2006;281:14361-9.
37. Xu W, Yuan X, Xiang Z, Mimnaugh E, Marcu M, Neckers L. Surface charge and hydrophobicity determine ErbB2 binding to the Hsp90 chaperone complex. Nat Struct Mol Biol. 2005;12:120-6.
38. Gherardi E, Birchmeier W, Birchmeier C, Vande Woude G. Targeting MET in cancer: rationale and progress. Nat Rev Cancer. 2012;12:89-103.
39. Schmidt L, Junker K, Nakaigawa N, Kinjerski T, Weirich G, Miller M, et al. Novel mutations of the MET proto-oncogene in papillary renal carcinomas. Oncogene. 1999;18:2343-50.
40. Kobayashi S, Boggon TJ, Dayaram T, Janne PA, Kocher O, Meyerson M, et al. EGFR mutation and resistance of non-small-cell lung cancer to gefitinib. N Engl J Med. 2005;352:786-92.
41. Engelman JA, Zejnullahu K, Mitsudomi T, Song Y, Hyland C, Park JO, et al. MET amplification leads to gefitinib resistance in lung cancer by activating ERBB3 signaling. Science. 2007;316:1039-43.
42. Shimamura T, Li D, Ji H, Haringsma HJ, Liniker E, Borgman CL, et al. Hsp90 inhibition suppresses mutant EGFR-T790M signaling and overcomes kinase inhibitor resistance. Cancer Res. 2008;68:5827-38.
43. Katayama R, Khan TM, Benes C, Lifshits E, Ebi H, Rivera VM, et al. Therapeutic strategies to overcome crizotinib resistance in non-small cell lung cancers harboring the fusion oncogene EML4-ALK. Proc Natl Acad Sci U S A. 2011;108:7535-40.
44. Pashtan I, Tsutsumi S, Wang S, Xu W, Neckers L. Targeting Hsp90 prevents escape of breast cancer cells from tyrosine kinase inhibition. Cell Cycle. 2008;7:2936-41.
45. Wang S, Pashtan I, Tsutsumi S, Xu W, Neckers L. Cancer cells harboring MET gene amplification activate alternative signaling pathways to escape MET inhibition but remain sensitive to Hsp90 inhibitors. Cell Cycle. 2009;8:2050-6.
46. Sang J, Acquaviva J, Friedland JC, Smith DL, Sequeira M, Zhang C, et al. Targeted Inhibition of the Molecular Chaperone Hsp90 Overcomes ALK Inhibitor Resistance in Non-Small Cell Lung Cancer. Cancer Discov. 2013;3:430-43.
47. George P, Bali P, Cohen P, Tao J, Guo F, Sigua C, et al. Cotreatment with

17-allylamino-demethoxygeldanamycin and FLT-3 kinase inhibitor PKC412 is highly effective against human acute myelogenous leukemia cells with mutant FLT-3. Cancer Res. 2004;64:3645-52.

48. Taipale M, Krykbaeva I, Koeva M, Kayatekin C, Westover KD, Karras GI, et al. Quantitative analysis of HSP90-client interactions reveals principles of substrate recognition. Cell. 2012;150:987-1001.

49. Polier S, Samant RS, Clarke PA, Workman P, Prodromou C, Pearl LH. ATP-competitive inhibitors block protein kinase recruitment to the Hsp90-Cdc37 system. Nat Chem Biol. 2013.

50. Radujkovic A, Schad M, Topaly J, Veldwijk MR, Laufs S, Schultheis BS, et al. Synergistic activity of imatinib and 17-AAG in imatinib-resistant CML cells overexpressing BCR-ABL--Inhibition of P-glycoprotein function by 17-AAG. Leukemia. 2005;19:1198-206.

Figure legends

Figure 1. MET is a client protein of HSP90.

A, Interaction between endogenous wild type MET and HSP90. MKN45 cells were lysed and subjected to immunoprecipitation (IP) with anti-MET antibody followed by immunoblotting with anti-HSP90 and anti-MET antibodies. Immunoprecipitation with immunoglobulin G (IgG) was used as a negative control. Input represents 5% of the total protein extract used for IP.

B, Phosphorylated wild type MET preferentially interacts with HSP90. NIH3T3 cells stably expressing wild type MET were incubated in medium supplemented with ('+') or without ('-') serum including HGF. After 24 h, cells were lysed and subjected to immunoprecipitation (IP) with anti-MET antibody and blotted with indicated antibodies.

C, Dose and time response of wild type MET and phosphorylated wild type MET to HSP90 inhibitor. MKN45 cells were incubated with increasing concentrations of geldanamycin (GA) for 24 h (left panel), and incubated for increasing time intervals with 0.5 μM GA (right panel). Cells were collected and subjected to immunoblotting. α-tubulin was used as loading control.

D, GA-stimulated wild type MET degradation is mediated by the proteasome. MKN45 cells were treated with the proteasome inhibitor MG132 (10 μM) 1 h before treatment with 0.5 μM GA for an additional 8 h. Cells were collected, lysed and subjected to immunoblotting.

E, HSP90 inhibition results in enhanced wild type MET ubiquitination. MKN45 cells were treated with MG132 (10 μM) 1 h before treatment with 0.5 μM GA for an additional 4 h. Cells were collected, lysed and subjected to immunoprecipitation (IP) with anti-MET antibody followed by immunoblotting with anti-poly-ubiquitin and

anti-MET antibodies.

Figure 2. Activated MET depends on HSP90 association for its stability.

A, Constitutively active mutant MET strongly interacts with HSP90. NIH3T3 cells stably expressing wild type (wt) MET or constitutively active mutant MET (Y1248H) were lysed and subjected to immunoprecipitation (IP) with anti-MET antibody followed by immunoblotting with anti-HSP90, anti-MET and anti-p-MET antibodies.

B, Constitutively active mutant MET is more sensitive to HSP90 inhibition than is wtMET. NIH3T3 cells stably expressing wtMET or constitutively active mutant MET (Y1248H) were incubated in medium supplemented with serum including HGF and increasing concentrations of GA for 24 h. Cells were collected and subjected to immunoblotting with indicated antibodies.

C, Alignment of the amino acid sequence of MET and EGFR kinase domain αC-β4 loops. Amino acid sequences (in one-letter code) of MET and EGFR in the αC-β4 loops were aligned by using MacVector software. Star denotes identity, and dot denotes similarity. Residues that differ between MET and EGFR are shaded; MET/EGFR denotes MET with highlighted residues from EGFR. Amino acid residues in MET and EGFR are numbered from the starting methionine.

D, MET-Y1248H/EGFR loses association with HSP90. Expression vectors encoding V5-tagged MET-Y1248H, MET-Y1248H/EGFR or an empty vector (pcDNA, used as a control) were transfected into HEK293 cells. After 48 h, cells were lysed and subjected to immunoprecipitation (IP) with anti-V5 antibody followed by immunoblotting with anti-HSP90, anti-V5 and anti-p-MET antibodies.

E, Steady-state phosphorylation of MET-Y1248H/EGFR is reduced compared to MET-Y1248H. Expression vectors encoding V5-tagged MET-Y1248H,

MET-Y1248H/EGFR or an empty vector (pcDNA) were transfected into HEK293 cells. After 48 h, cells were lysed and subjected to immunoblotting as shown.

F, MET-Y1248H/EGFR retains HGF sensitivity. HEK293 cells were transfected with V5-tagged empty plasmid, wtMET, or MET-Y1248H/EGFR (2 μg each). After 48 h, cells were serum-starved overnight and then treated for 20 min with 1 nM HGF. Samples were then lysed in buffer (20 mM Hepes, 100 mM NaCl, 1 mM $MgCl_2$, 0.1% NP-40, 20 mM Na_2MoO_4, phosphatase and protease inhibitors). Equal amounts of total cell lysate were resolved by Western blotting and probed with indicated antibodies. After normalization to total MET protein, HGF increased the activated fraction of wtMET 4.8-fold and the activated fraction of MET-Y1248H/EGFR 8.9-fold (by densitometric analysis).

G, HEK293 cells were transfected as in *F*, treated with HGF and exposed to increasing concentrations of crizotinib (16 h). MET-Y1248H/EGFR, which displays reduced interaction with Hsp90, is markedly more sensitive to the TKI compared to MET-Y1248H.

Figure 3. MET TKI and HSP90 inhibitor synergize in wild type MET-overexpressing cells.

A, HSP90 inhibitor enhances the efficacy of MET TKI on wtMET phosphorylation and downstream signaling. MKN45 cells (left panel) and H1993 cells (right panel) were treated for 16 h with increasing concentrations of crizotinib alone or in combination with the indicated concentrations of ganetespib, lysed and subjected to immunoblotting as shown.

B-C, Combination of crizotinib and ganetespib synergistically inhibits wtMET-driven cell growth. MKN45 cells were treated with increasing concentrations of crizotinib

alone or in combination with the indicated concentrations of ganetespib for 48 h and subjected to MTT assay (B). Data are expressed as mean ± SD of triplicate experiments. Combination index (CI) was calculated to examine the synergistic effect of these drugs (C). CI values < 1 indicate synergy, whereas CI > 1 indicates antagonism between two drugs.

D, Synergistic growth inhibition is due to G1 arrest. MKN45 cells were treated with the indicated concentrations of crizotinib alone or in combination with 10 nM ganetespib for 48 h and subjected to cell cycle analysis.

E, Combination treatment dramatically inhibits soft agar colony growth of wtMET overexpressing cells. MKN45 cells were plated in 0.4% soft agar with indicated drugs, either alone or in combination, and cultures were maintained for 3 weeks. Representative images of colonies are shown for each condition (*Scale bar,* 0.1 mm); colonies with a diameter of > 0.1 mm were counted microscopically and graphed. Data are means ± SD of triplicate experiments. *, $P < 0.05$ vs. control (unpaired Student's *t*-test followed by Bonferroni test).

Figure 4. MET kinase domain mutants retain sensitivity to HSP90 inhibition.

A, Ganetespib inhibits MET phosphorylation and downstream signaling in TKI-sensitive MET mutants. NIH3T3 cells stably expressing TKI-sensitive MET mutants (V1238I and H1112Y) were treated for 16 h with increasing concentrations of either crizotinib or ganetespib, lysed and subjected to immunoblotting.

B, Ganetespib inhibits MET phosphorylation and downstream signaling in TKI-resistant MET mutants. NIH3T3 cells stably expressing TKI-resistant MET mutants (Y1248H and L1213V) were treated and analyzed as described above.

Figure 5. MET TKI and HSP90 inhibitor synergize in TKI-resistant MET

mutant-expressing cells.

A, NIH3T3 cells stably expressing TKI-resistant MET-Y1248H (left panel) or MET-L1213V (right panel) were exposed to increasing concentrations of crizotinib in the presence or absence of defined concentrations of ganetespib, lysed and subjected to immunoblotting.

B, Soft agar colony growth of NIH3T3 cells stably expressing TKI-resistant MET-Y1248H was assessed and analyzed as described in Figure 3E.

C, Combination treatment dramatically inhibits invasion of TKI-resistant mutant MET-expressing cells. NIH3T3 cells stably expressing TKI-resistant mutant MET-Y1248H in serum-free medium containing indicated drugs were added to upper wells of transwell chambers. The membrane separating upper and lower wells was coated with matrigel. Lower wells contained medium with 10% FBS as chemo-attractant. After 48 h, invaded cells (e.g., cells appearing on the lower surface of the separating membrane) were stained and counted microscopically. Data are shown as mean ± SD of triplicate experiments. *, $P < 0.05$ vs. control (unpaired Student's *t*-test followed by Bonferroni test).

Figure 6. MET TKI and HSP90 inhibitor synergistically inhibit tumor growth in MET-driven xenograft tumor models.

A-B, Combination of sub-optimal concentrations of crizotinib and ganetespib displays significantly greater efficacy compared to either drug alone in MET-driven xenograft tumor models. Athymic mice bearing established MKN45 xenografts (A), or NIH3T3 xenografts stably expressing TKI-resistant mutant MET-Y1248H (B) were administered crizotinib once daily and ganetespib three times per week, either as single agents or concurrently for 3 weeks (A) or 2 weeks (B). Tumor volume was measured using

calipers on indicated days; data are shown as mean ± SD (n=6/group). Percent tumor growth values were calculated on the final day of study by comparing tumor volumes in drug-treated and vehicle-treated mice. *, $P < 0.05$ vs. control (unpaired Student's *t*-test followed by Bonferroni test). Average body weight changes were measured over the course of the study (A-B, lower graphs).

C-D, Pharmacodynamic assessment of the treatment regimens described in panels A and B. Tumors were resected on the final day of the study 6 h post drug administration, and subjected to immunoblotting as shown. Tubulin was used to demonstrate equal protein per sample.

Miyajima et al., Figure 1

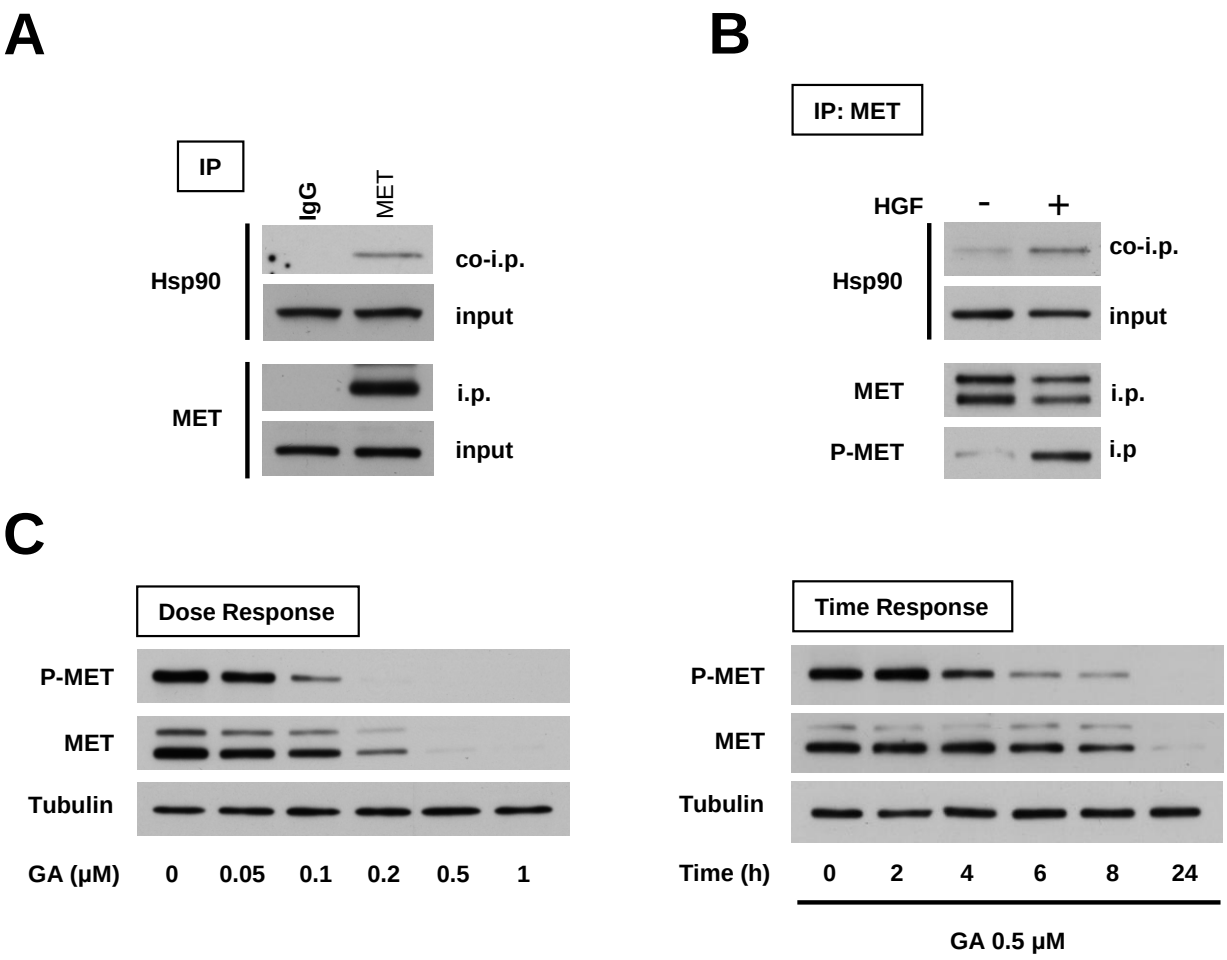

Miyajima et al., Figure 2

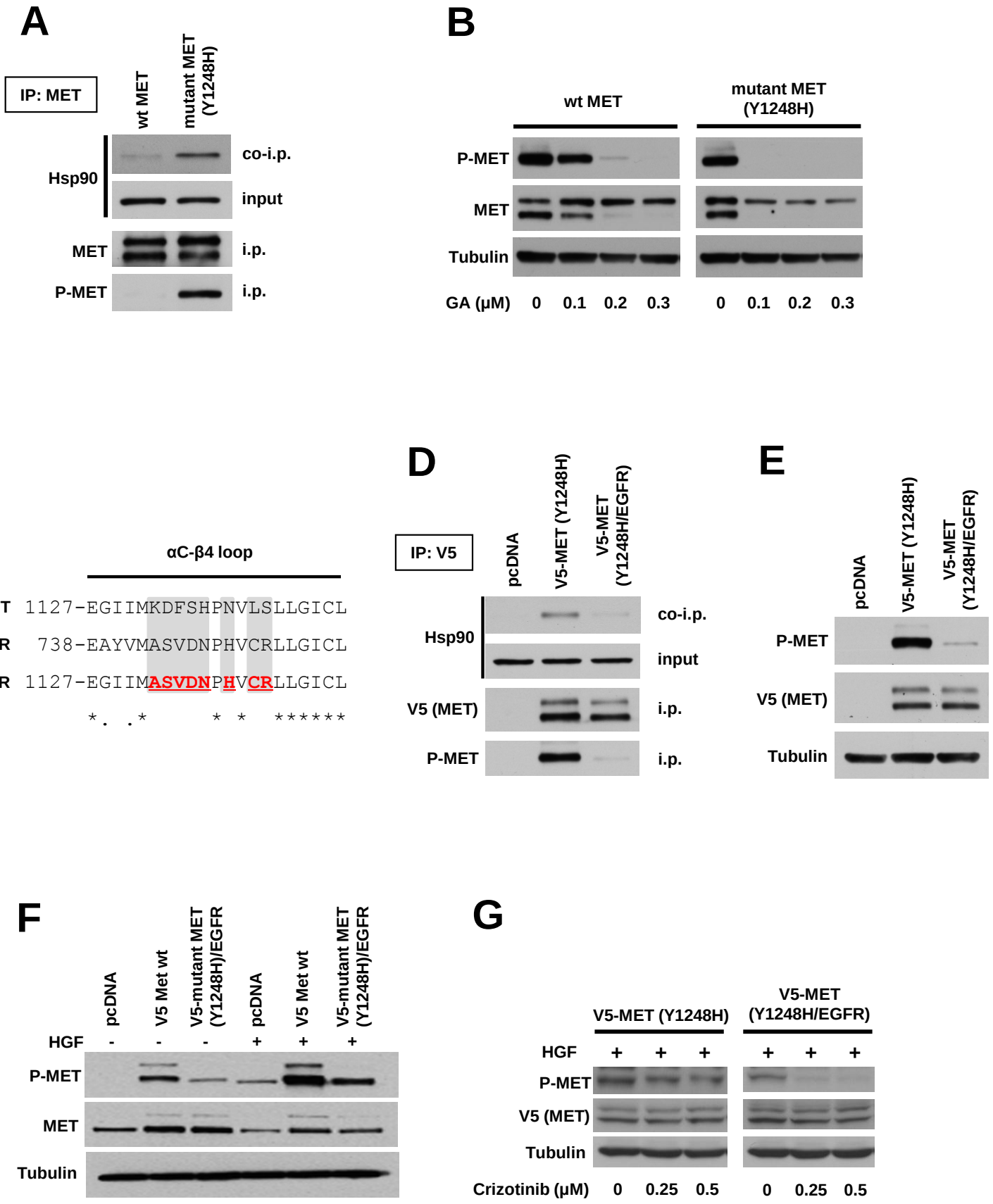

Miyajima et al., Figure 3

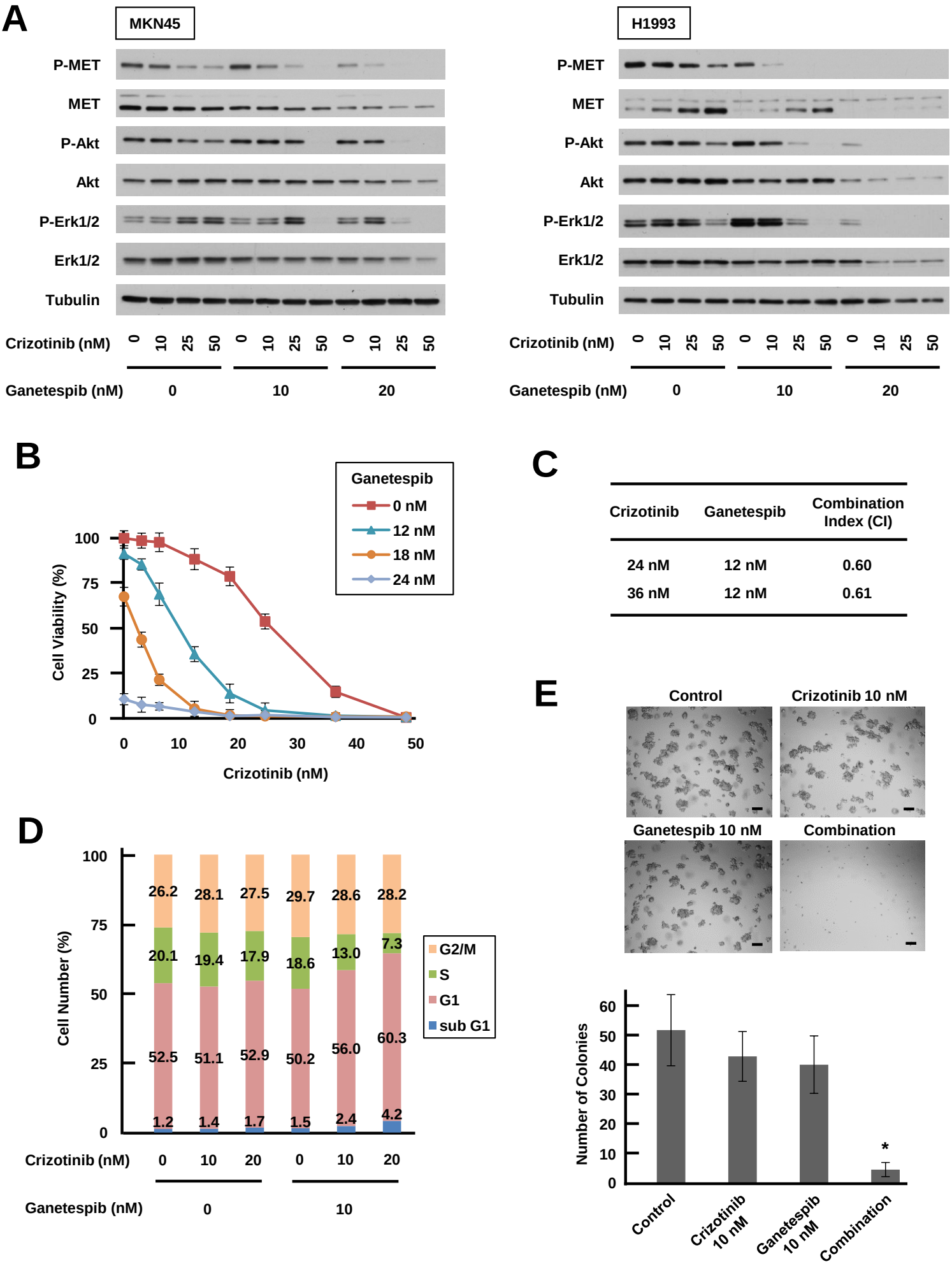

Miyajima et al., Figure 4

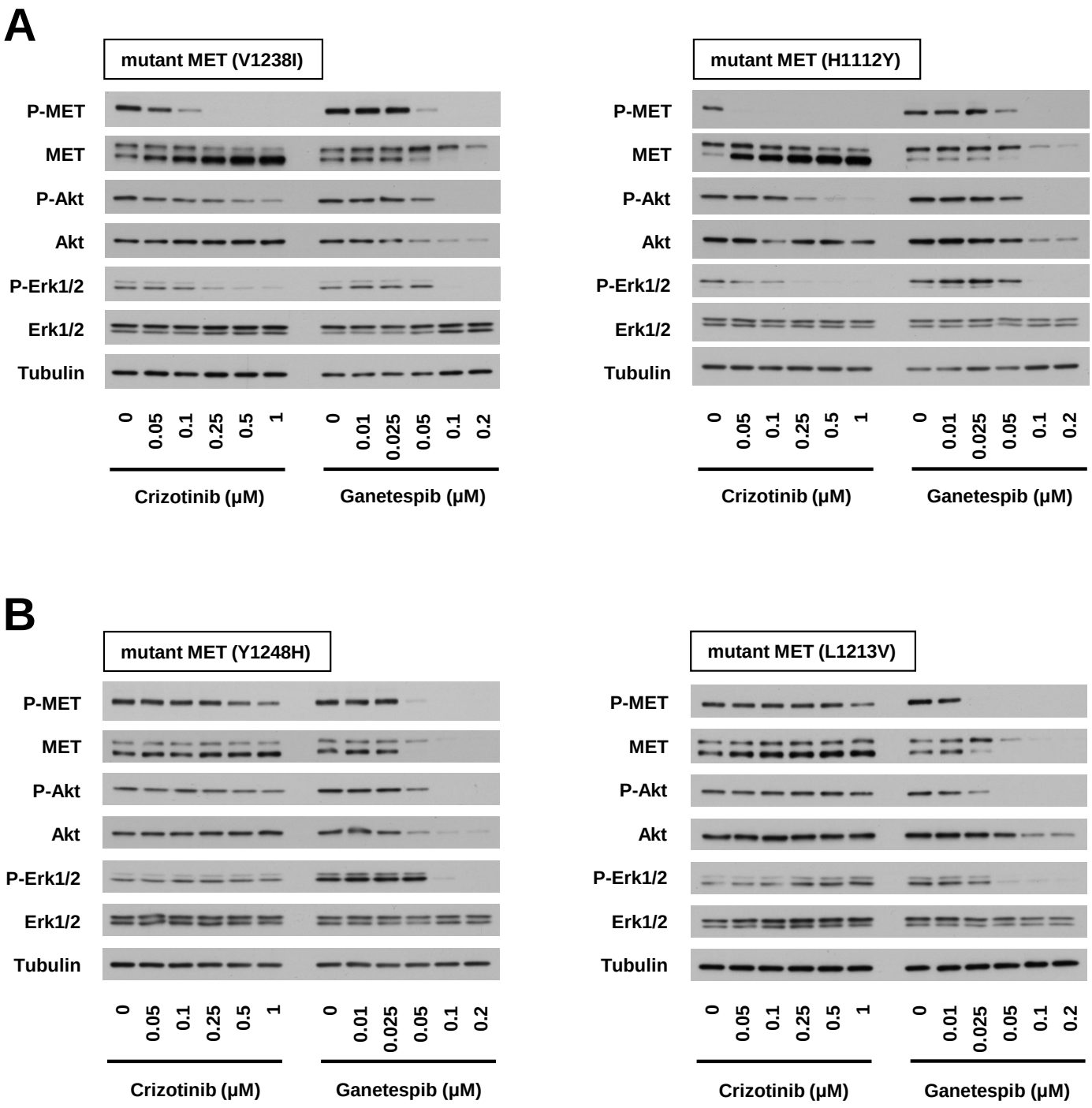

Miyajima et al., Figure 5

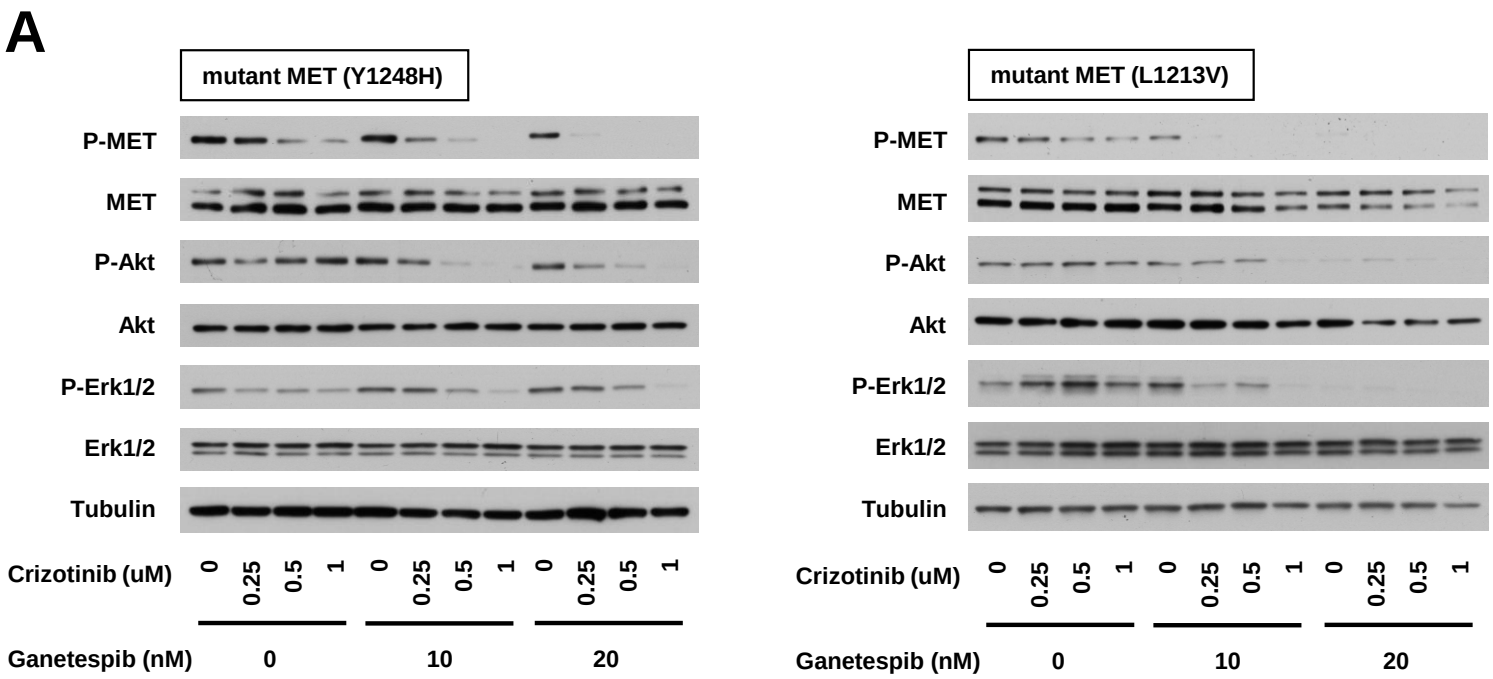

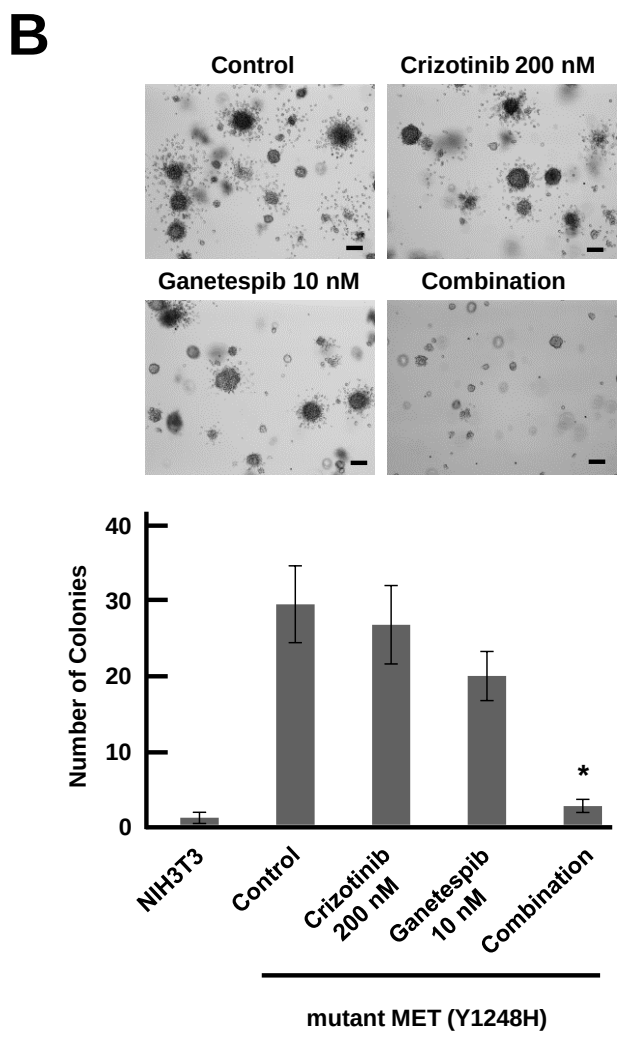

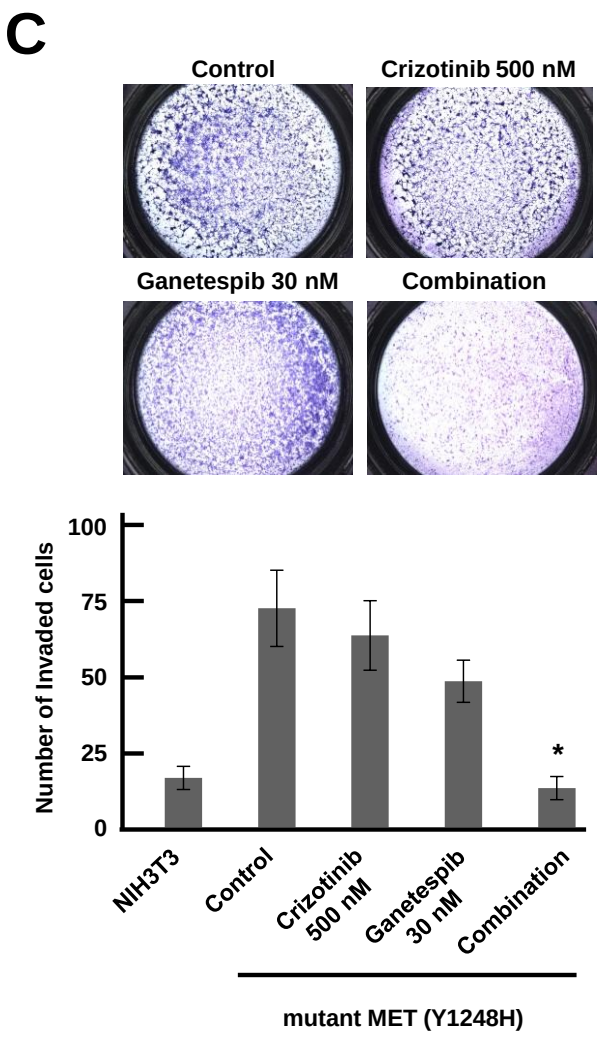

Miyajima et al., Figure 6

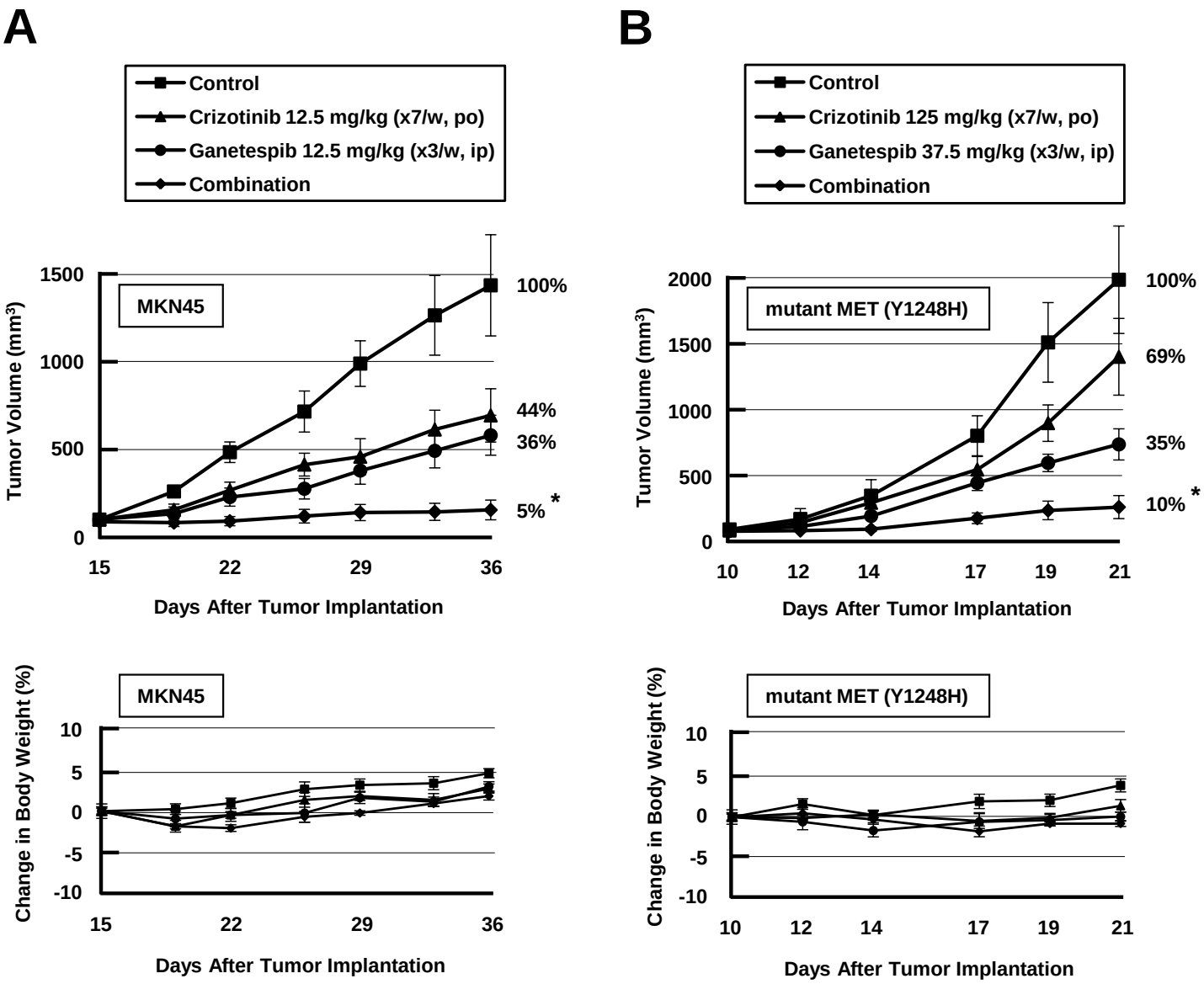

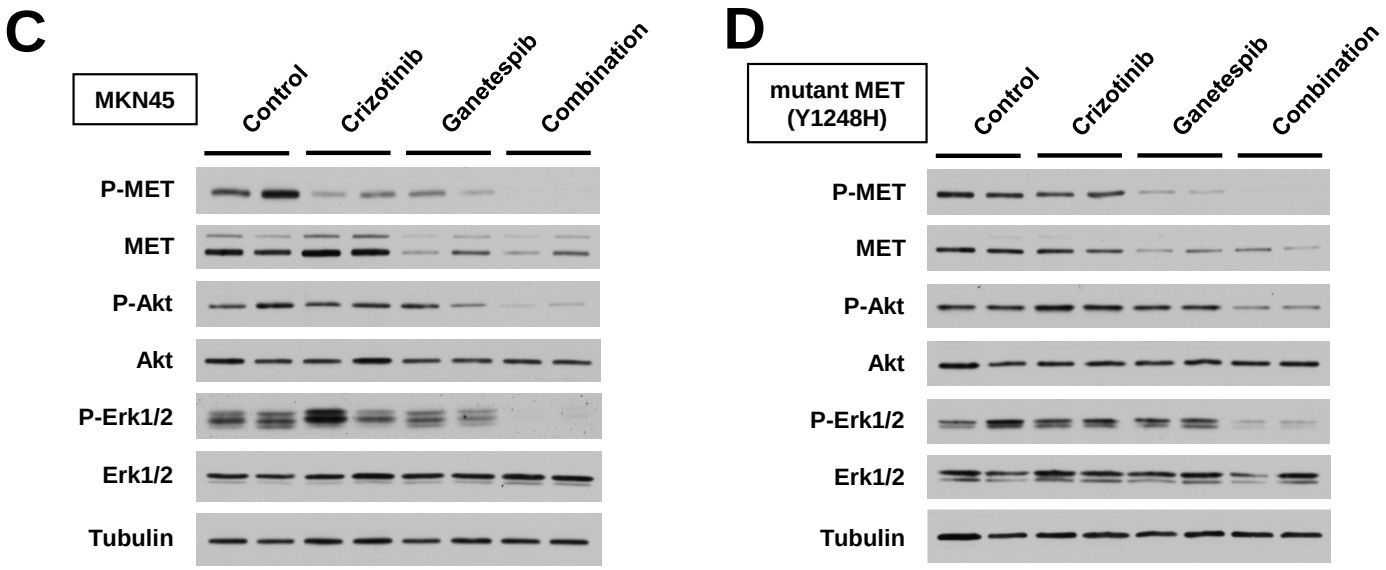

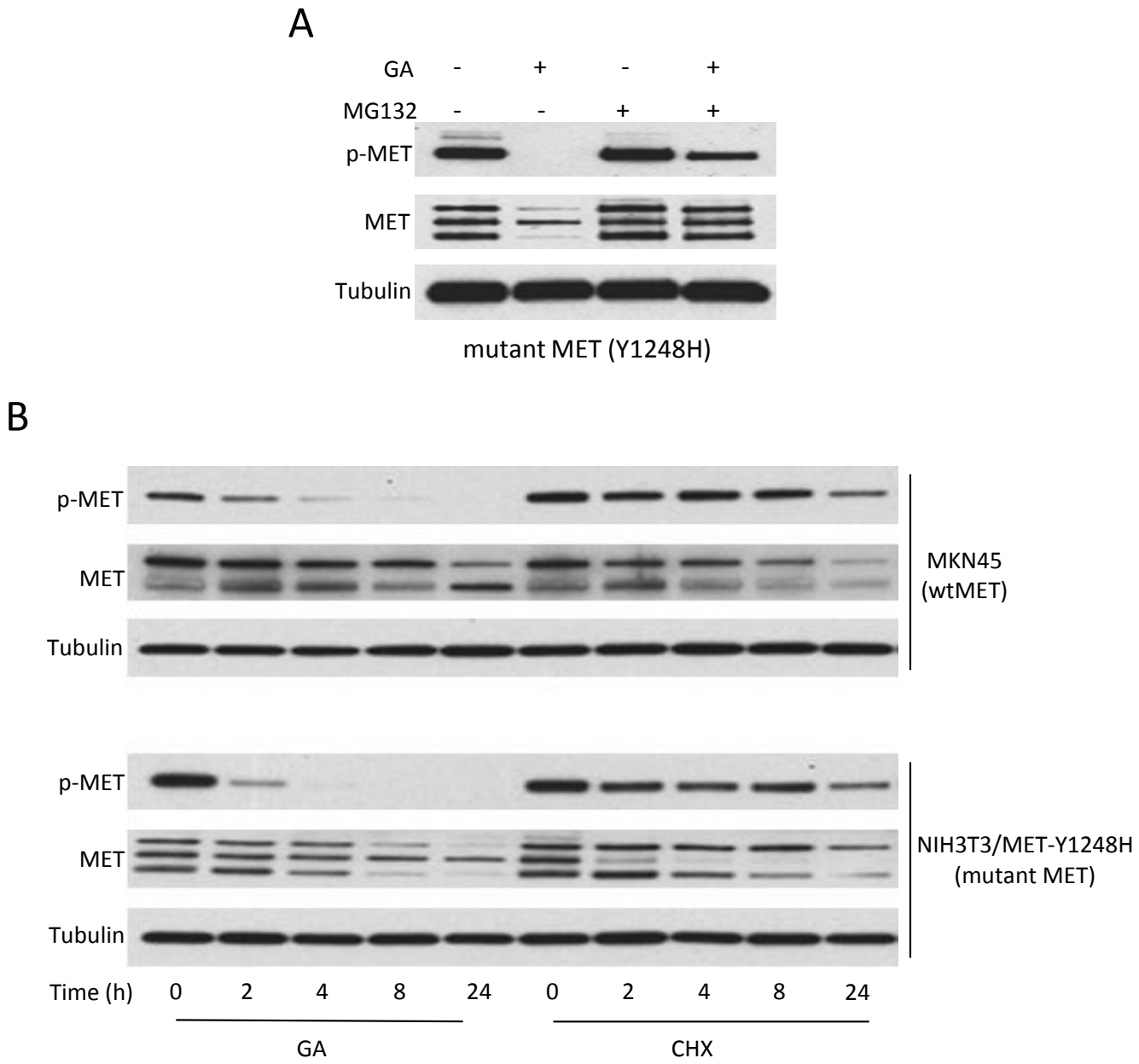

Miyajima et al., Figure S1

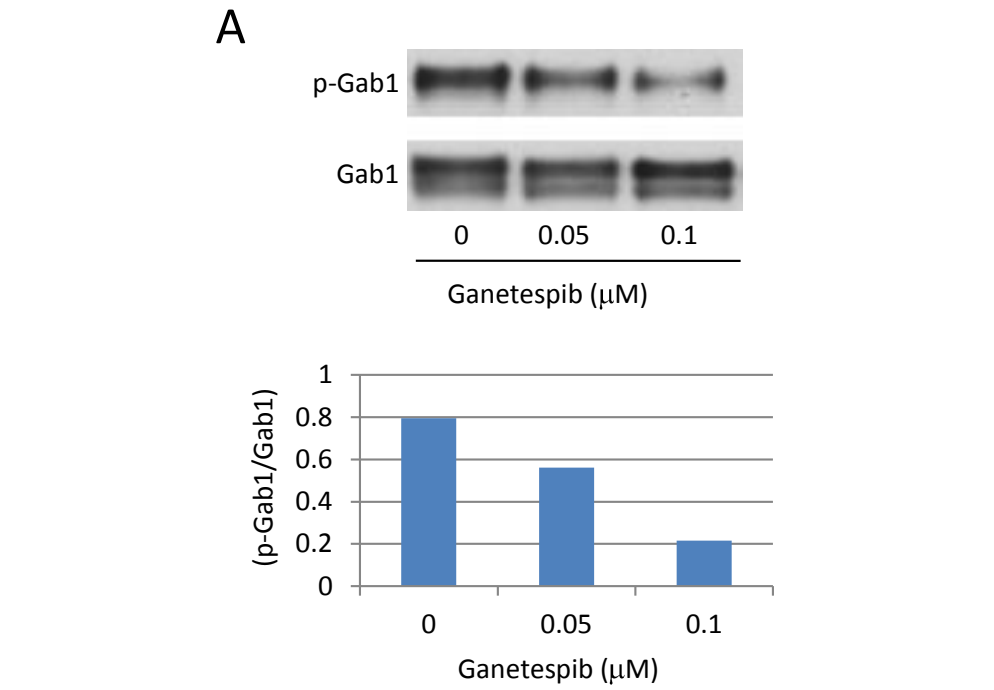

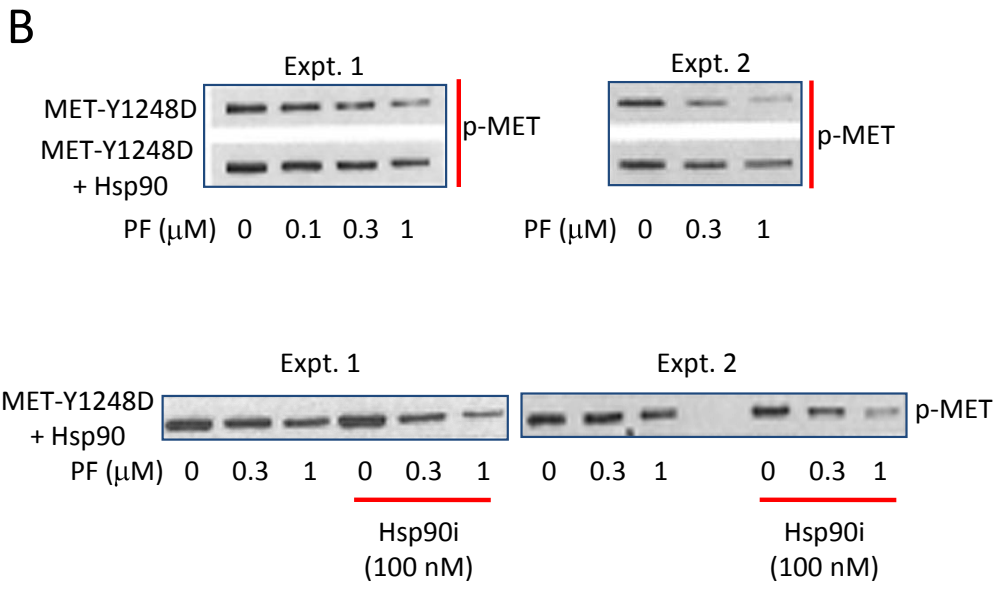

Miyajima et al., Figure S2

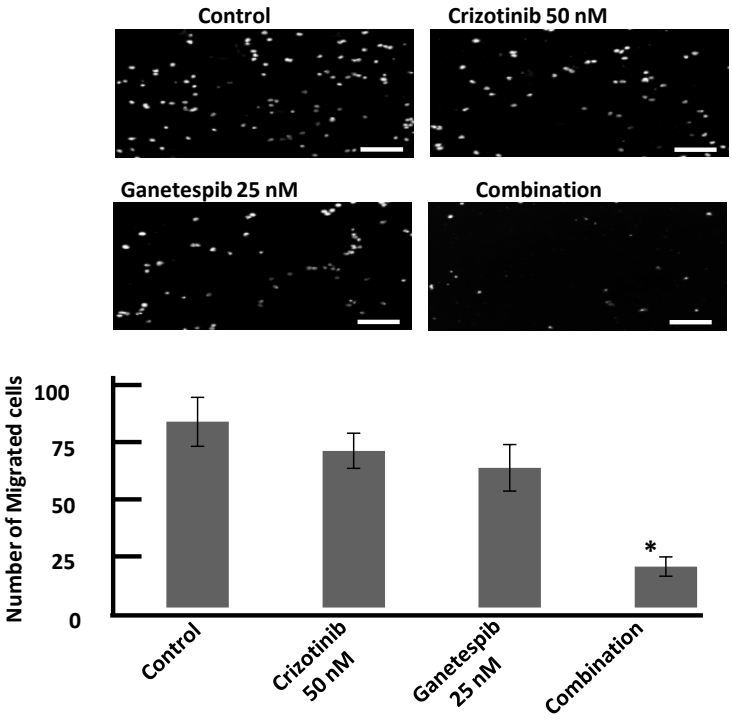

Miyajima et al., Figure S3

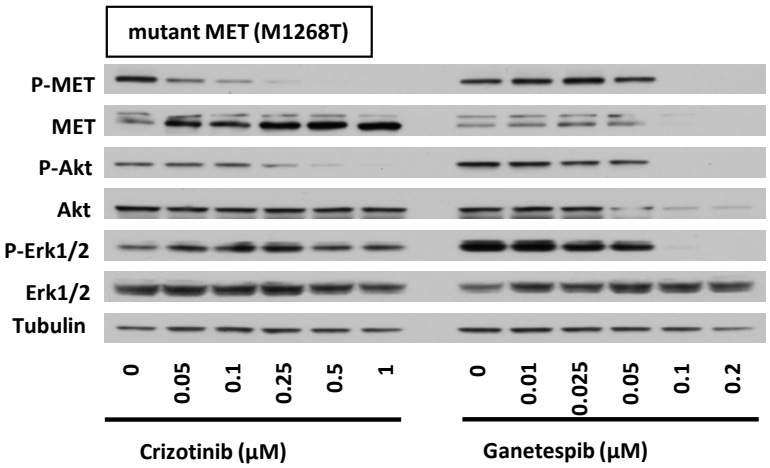

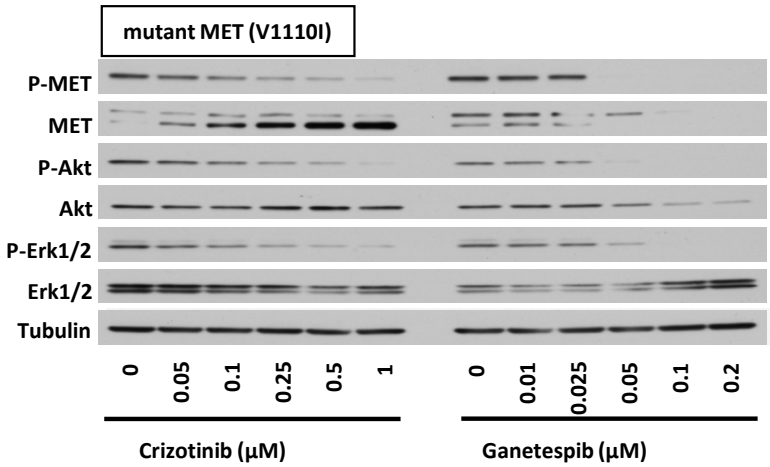

Miyajima et al., Figure S4

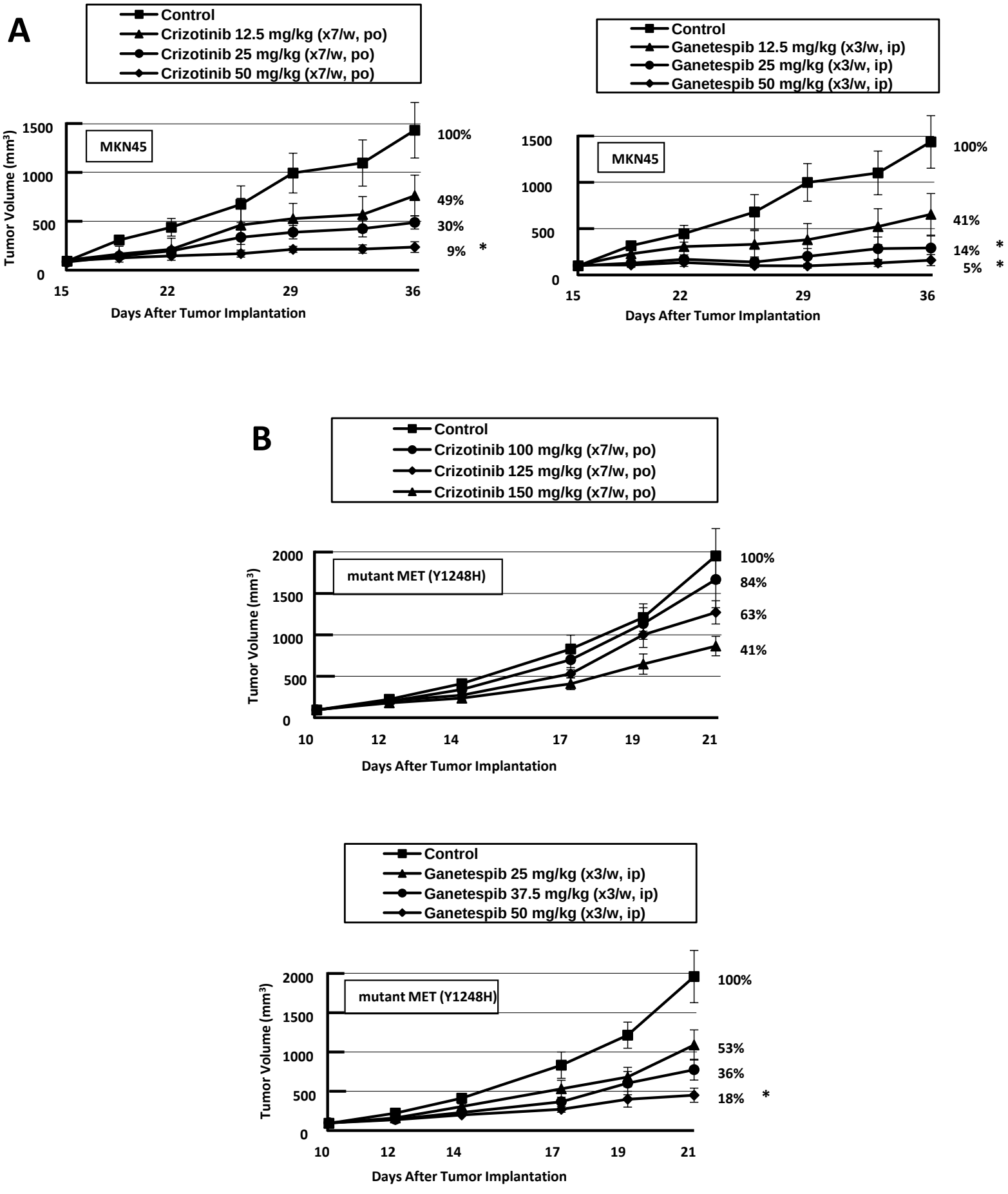

Miyajima et al., Figure S5

Supplemental Tables and Figure Legends

Supplemental Table 1. Combination index (CI) was calculated (as in Figure 3C) to examine whether crizotinib and ganetespib synergized to inhibit soft agar colony growth of NIH3T3 cells stably expressing TKI-resistant MET-Y1248H. A CI value < 1 indicates synergy.

Crizotinib (nM)	Ganetespib (nM)	Combination Index (CI)
150	10	0.81
200	10	0.73

Supplemental Table 2. Crizotinib and ganetespib synergistically reduce growth of wild-type and mutant MET-driven tumor xenografts. Relative tumor volumes of control and treated groups on the final day of the study shown in Fig. 6A, B were determined. Combination therapy had a greater than additive effect on tumor growth inhibition in both MKN45 (wild-type MET) and NIH3T3/MET-Y1248H xenografts. [a] FTV, fractional tumor volume, calculated as mean tumor volume experimental/mean tumor volume control. [b] Mean FTV of crizotinib-treated mice x mean FTV of ganetespib-treated mice. [c] Obtained by dividing the expected FTV by the observed FTV. A ratio > 1 indicates synergy; a ratio < 1 indicates a less than additive effect of the drug combination.

Fractional tumor volume (FTV) relative to untreated controls[a]					
Xenograft	Crizotinib	Ganetespib	Expected[b]	Observed	Ratio expected FTV/observed FTV[c]
MKN45	0.52	0.45	0.23	0.12	1.86
NIH3T3/MET (Y1248H)	0.71	0.36	0.25	0.15	1.61

Supplemental Figure Legends

Supplemental Figure 1. *A*, NIH3T3/MET-Y1248H cells were treated with MG132 (10 μM) 1h before treatment with 0.5 μM GA for an additional 8 h. Cells were collected, lysed in TNES buffer (50 mM Tris-HCl pH 7.5, 1% NP-40, 2 mM EDTA, 100 mM NaCl, plus protease and phosphatase inhibitors) and subjected to immunoblotting. *B*, MKN45 and NIH3T3/MET-Y1248H cells were treated with either 0.5 μM GA or 100 μg/ml cycloheximide for the indicated times and then lysed in TNES buffer. Equal amounts of total protein from each sample were subjected to immunoblotting.

Supplemental Figure 2. *A*, NIH3T3/MET-Y1248H cells were treated with indicated concentrations of ganetespib (16 h), then lysed in TNES buffer and subjected to immunoblotting. *B*, Inclusion of bacterially purified Hsp90 protein (50 nM) with bacterially purified, constitutively active MET-Y1248D protein (50 nM, Millipore) inhibits sensitivity to crizotinib ('PF') in an *in vitro* kinase assay (top 2 panels); pre-incubation with GA (100 nM) restores sensitivity to crizotinib (bottom 2 panels). Briefly, proteins were resuspended in kinase buffer (50 mM Tris-HCl pH 7.5, 10 mM $MgCl_2$, 0.1 mM EDTA, 2 mM DTT). The kinase reaction was initiated by adding 0.2 mM ATP and incubating at 30˚C for 15 min. Kinase activity was assessed by visualizing MET autophosphorylation with appropriate antibodies.

Supplemental Figure 3. Combination of crizotinib and ganetespib inhibits migration of wtMET-overexpressing cells. MKN45 cells in serum-free medium containing indicated drugs were added to upper wells of transwell chambers. After 48 h, migrated cells (e.g., cells appearing on the lower surface of the uncoated separating membrane) were stained and counted microscopically. *Scale bar,* 0.1mm. Data are graphically displayed as mean ± SD of triplicate experiments. *, $P < 0.05$ vs. control (unpaired Student's *t*-test followed by Bonferroni test).

Supplemental Figure 4. Ganetespib inhibits MET phosphorylation and downstream signaling in NIH3T3 cells expressing the TKI-sensitive MET mutants M1268T or V1110I. Cells were treated, lysed and analyzed as described in Figure 4.

Supplemental Figure 5. *A*, A dose range study of single agent crizotinib or ganetespib in wtMET-driven xenografts. Athymic mice bearing MKN45 tumors were administered either crizotinib or ganetespib at the indicated dose and schedule for 3 weeks. Tumor volume was measured as described in Figure 6. Data are shown as mean ± SD (n=5/group). *, $P < 0.05$ vs. control (unpaired Student's *t*-test followed by Bonferroni test). *B*, A dose range study of single agent crizotinib or ganetespib in TKI-resistant MET-Y1248H-driven xenografts. Athymic mice bearing NIH3T3 tumors stably expressing MET-Y1248H were administered either crizotinib or ganetespib at the indicated dose and schedule for 2 weeks. Tumor volume was measured as described in Figure 6. Data are shown as mean ± SD (n=5/group). *, $P < 0.05$ vs. control (unpaired Student's *t*-test followed by Bonferroni test).